

# Atomic Layer Deposition of Silicon Nitride from Bis(*tert*-butylamino)silane and N<sub>2</sub> Plasma

Harm C. M. Knoops,<sup>\*,†,‡</sup> Eline M. J. Braeken,<sup>†</sup> Koen de Peuter,<sup>†</sup> Stephen E. Potts,<sup>§</sup> Suvi Haukka,<sup>||</sup> Viljami Pore,<sup>||</sup> and Wilhelmus M. M. Kessels<sup>\*,†</sup>

<sup>†</sup>Eindhoven University of Technology, P.O. Box 513, 5600 MB Eindhoven, Netherlands

<sup>‡</sup>Oxford Instruments Plasma Technology, North End, Bristol BS49 4AP, U.K.

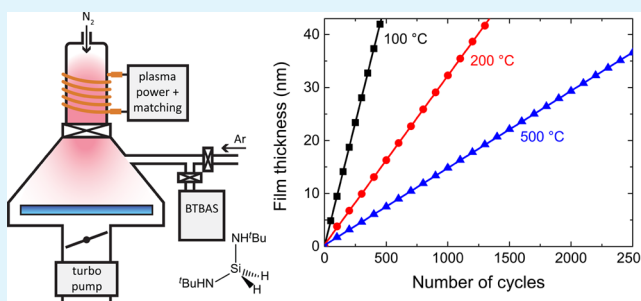
<sup>§</sup>Queen Mary University of London, Mile End Road, London E1 4NS, U.K.

<sup>||</sup>ASM, Pietari Kalmin katu 1 F 2, 00560 Helsinki, Finland

## Supporting Information

**ABSTRACT:** Atomic layer deposition (ALD) of silicon nitride (SiN<sub>x</sub>) is deemed essential for a variety of applications in nanoelectronics, such as gate spacer layers in transistors. In this work an ALD process using bis(*tert*-butylamino)silane (BTBAS) and N<sub>2</sub> plasma was developed and studied. The process exhibited a wide temperature window starting from room temperature up to 500 °C. The material properties and wet-etch rates were investigated as a function of plasma exposure time, plasma pressure, and substrate table temperature. Table temperatures of 300–500 °C yielded a high material quality and a composition close to Si<sub>3</sub>N<sub>4</sub> was obtained at 500 °C (N/Si = 1.4 ± 0.1, mass density = 2.9 ± 0.1 g/cm<sup>3</sup>, refractive index = 1.96 ± 0.03). Low wet-etch rates of ~1 nm/min were obtained for films deposited at table temperatures of 400 °C and higher, similar to that achieved in the literature using low-pressure chemical vapor deposition of SiN<sub>x</sub> at >700 °C. For novel applications requiring significantly lower temperatures, the temperature window from room temperature to 200 °C can be a solution, where relatively high material quality was obtained when operating at low plasma pressures or long plasma exposure times.

**KEYWORDS:** ALD, Si<sub>3</sub>N<sub>4</sub>, plasma, thin film, wet etch, atomic layer deposition, plasma-assisted ALD, silicon nitride



## INTRODUCTION

Silicon nitride (SiN<sub>x</sub>) is one of the most widely used thin-film materials, with a very extensive range of applications. However, the requirements on the material properties and on the growth control of these films are becoming ever more stringent. One method for the deposition of high-quality thin films with excellent growth control is atomic layer deposition (ALD). However, there are currently few reports on the ALD of silicon nitride. One application that could benefit greatly from a silicon nitride ALD process is gate spacers for high-*k* metal gate transistors.<sup>1</sup> These spacer films should serve as oxygen barrier and barrier to processing conditions and also provide a constant spacing of the source and the drain of the transistor, independent of transistor pitch. The films should therefore have a good etch resistance and have a high conformality.<sup>1,2</sup> Because of shrinking device features and the adoption of new materials, the associated allowed thermal budget during processing is also decreasing and the spacers have to be deposited at low temperatures (e.g., below 500 °C), while the film quality has to remain high.<sup>1</sup> For the ALD of SiN<sub>x</sub>, chlorosilanes (e.g., SiCl<sub>4</sub>, SiH<sub>2</sub>Cl<sub>2</sub>, Si<sub>2</sub>Cl<sub>6</sub>, and Si<sub>3</sub>Cl<sub>8</sub>) have generally been used as the silicon precursor in combination with coreactants such as NH<sub>3</sub>, NH<sub>3</sub> plasma, or N<sub>2</sub>H<sub>4</sub>.<sup>3–9</sup>

However, processes using chlorosilanes require relatively high deposition temperatures and can be undesirable because of detrimental effects caused by the chlorine in these precursors.<sup>10</sup> Therefore, a chlorine-free process is highly desired. As with other nitride ALD processes, plasmas can be employed as coreactant to increase the coreactant's reactivity.<sup>11</sup> Nonetheless, even with the high reactivity afforded by the plasma exposure, long plasma times are typically required to avoid high impurity contents. Recently, plasma ALD processes using chlorine-free precursors (i.e., SiH<sub>4</sub> and N(SiH<sub>3</sub>)<sub>3</sub>) have been reported using N<sub>2</sub> plasma or NH<sub>3</sub> plasma as coreactant, respectively.<sup>12,13</sup>

In this work, a novel ALD process using bis(*tert*-butylamino)silane (BTBAS) and N<sub>2</sub> plasma was developed and studied. High-quality SiN<sub>x</sub> was obtained, as evidenced by a low wet-etch rate of the material. First, the experimental details will be discussed. Second, the **Results** section discusses the film growth, as well as the effect of temperature and plasma exposure time. The wet-etch rates of the films are also presented. In the **Discussion** section, the main trends in film

Received: July 27, 2015

Accepted: August 25, 2015

Published: August 25, 2015

composition and wet-etch rates are addressed, and a comparison is made with  $\text{SiN}_x$  ALD processes reported in the literature.

## EXPERIMENTAL DETAILS

Figure 1 shows a simplified schematic representation of the Oxford Instruments FlexAL reactor in which the depositions were carried

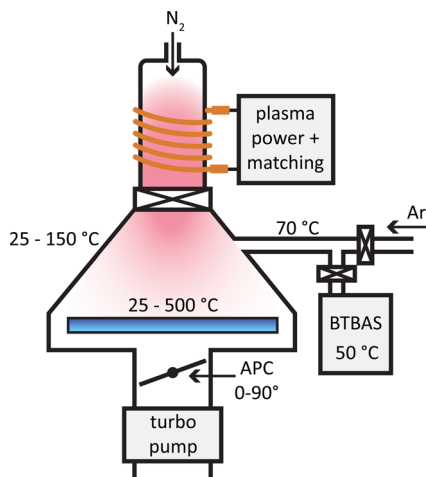


Figure 1. A simplified schematic of the ALD reactor used for deposition of  $\text{SiN}_x$ . The reactor comprises a chamber containing a heated substrate table; an inductively coupled plasma (ICP) source with  $\text{N}_2$  gas injection from the top; a precursor delivery system for BTBAS, which was vapor-drawn into a line that was purged by Ar; and a pumping system with a turbo pump and an automated pressure controller (APC) valve to control the effective pumping speed. Substrates with a diameter up to 200 mm were used. The temperatures employed during the experiments are indicated.

out.<sup>14</sup> The reactor is equipped with a remote inductively coupled (ICP) plasma generator, which was operated at 600 W at 13.56 MHz. The depositions were performed on c-Si substrates with a thin native oxide layer. No additional cleaning steps were used. Due to poor thermal contact in vacuum, actual wafer temperatures were lower than the set table temperature. See the Supporting Information for a table with the determined wafer temperature for each set-point table temperature.<sup>15</sup> In the remainder of this work the set-point table temperatures are reported. The chamber wall temperature was set to 150 °C, except for deposition temperatures below 150 °C for which the wall temperature was set to the deposition temperature. A base pressure in the reactor chamber of  $\sim 10^{-6}$  Torr was reached by a turbo pump. A butterfly valve in front of the turbo pump controlled the effective pumping speed and functions as an automated pressure controller (APC).  $\text{SiH}_2(\text{NH}^t\text{Bu})_2$  (BTBAS, purity  $\geq 98.5\%$ , Air Products Inc.) was used as the precursor and held at a bubbler temperature of 50 °C. The precursor was vapor drawn, where Ar (25 sccm, purity 99.999%) was used as a carrier gas in the line during precursor dosing and during the subsequent reaction step. For both steps the APC valve was set to 10° to reduce the effective pumping speed and maximize precursor usage. During the purging step after precursor dosing the Ar flow was 100 sccm. For both purging steps the APC valve was set to 90° valve position for maximum pumping. The delivery lines were heated to 70 °C to prevent precursor condensation. Based on the saturation curves for precursor dose and plasma exposure, the following recipe was chosen as a standard: 1 s delivery line purge, 150 ms BTBAS dose time, 3 s reaction time, 1 s precursor purge time, 2 s preplasma time, 10 s plasma exposure time, 100 sccm  $\text{N}_2$  flow plasma gas (purity 99.999%), 40 mTorr set plasma pressure, and 1 s plasma purge time. These settings were used unless mentioned otherwise.

The film thickness and optical properties of the layers were measured by spectroscopic ellipsometry (SE), using a J.A. Woollam Co. M-2000F ellipsometer over a wavelength range of 245–1000 nm. The optical model consisted of a silicon substrate,  $\sim 1.5$  nm native oxide, and a silicon nitride layer modeled with a Tauc-Lorentz dispersion relation. The chemical composition and stoichiometry of the  $\text{SiN}_x$  films were investigated with X-ray photoelectron spectroscopy (XPS), using a Thermo Scientific K-Alpha spectrometer with a monochromatic Al  $K\alpha$  X-ray source ( $h\nu = 1486.6$  eV). Depth profiles were measured by sputtering with  $\text{Ar}^+$  ions. Rutherford backscattering spectrometry (RBS) and elastic recoil detection (ERD) measurements were also used to determine the composition and mass density of the films. The RBS and ERD experiments and the simulations were performed by AccTec B.V using a 1.85 MeV helium-ion beam. Simulations were used to determine the areal densities of the elements.

For determining the wet-etch rates of the silicon nitride films, two types of HF solution were used: (1) a buffered HF solution composed of a 7:1 volume ratio of 40%  $\text{NH}_4\text{F}$  in water and 49% HF in water, referred to as 7:1 BHF, and (2) a nonbuffered 0.5% (0.25 mol/L) HF solution, referred to as 100:1 HF. The procedure for etching the films was as follows. First, the samples were placed in a holder that could hold multiple samples at once so no influence of different incubation or rinse times had to be taken into account. Second, the holder was immersed in the HF solution for a set time and subsequently rinsed in deionized water with resistance  $R > 10$  M $\Omega$ cm. After rinsing, the samples were blown dry with nitrogen gas and then characterized by SE. The steady-state etch rates were determined from linear regression of thickness measurements on at least three separate samples each with a different etch time.

## RESULTS

**Film Growth and Effect of Table Temperature.** Initial experiments showed that the use of H-containing plasmas (e.g.,  $\text{H}_2$ – $\text{N}_2$  plasmas or  $\text{NH}_3$  plasmas) led to very low growth-per-cycle (GPC) values of  $0.05 \pm 0.02$  Å at both 200 and 500 °C, and therefore only results from pure  $\text{N}_2$  plasmas will be reported in the remainder of this article. Note that termination by -H and -NH species of surface groups limiting BTBAS precursor adsorption is believed to be the main mechanism for this suppressed growth.<sup>16</sup> The  $\text{SiN}_x$  process with  $\text{N}_2$  plasma showed linear growth with no growth delay at all table temperatures (shown for 100, 200, and 500 °C in Figure 2). The thickness nonuniformity on an 8 in. wafer was typically less than 5%. In Table 1 the GPC and material properties are shown for films deposited at different table temperatures. Figure 3 shows the saturation curves for the precursor step for 100 °C, 200 °C, and 500 °C. Interestingly, over this entire temperature range the precursor showed saturating behavior with possibly a

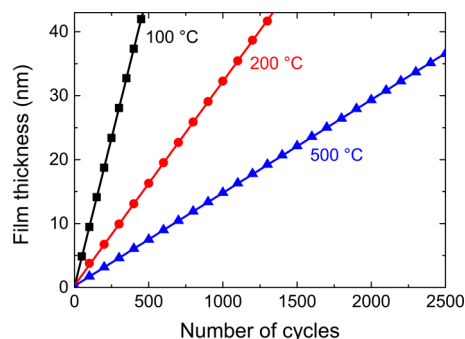
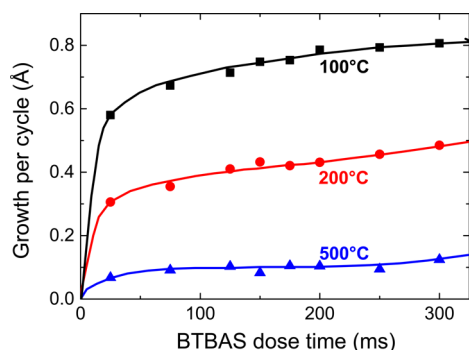


Figure 2. Film thickness as a function of the number of cycles measured with *in situ* spectroscopic ellipsometry for  $\text{SiN}_x$  films deposited at a table temperature of 100 °C, 200 °C, and 500 °C. The lines are linear fits to the data.

**Table 1.** Growth per Cycle (GPC), Refractive Index, Mass Density, and Elemental Composition of SiN<sub>x</sub> Films Deposited Using 10 s Plasma Exposure Time at 40 mTorr N<sub>2</sub> Pressure and Various Table Temperatures<sup>a</sup>

table temp (°C)	GPC (Å)	refractive index	RBS		XPS		ERD	
			mass density (g/cm <sup>3</sup> )	N/Si ratio	N/Si ratio	[C] at. %	[O] at. %	[H] at. %
100	0.93 ± 0.02	1.63 ± 0.03	-	-	2.7 ± 0.1	25 ± 1	3 ± 1	-
200	0.32	1.83	2.2 ± 0.1	2.0 ± 0.1	1.7	9	5	10.9 ± 0.5
300	0.21	1.92	2.8	1.6	1.6	4	5	8.3
400	0.16	1.96	2.8	1.5	1.5	2	4	5.4
500	0.15	1.96	2.9	1.4	1.5	2	5	5.0
bulk Si <sub>3</sub> N <sub>4</sub>	-	2.02	3.2	1.33	1.33	0	0	0

<sup>a</sup>Typical error margins are indicated for the first value in each column. A dash indicates “not measured”. The last row indicates the properties of bulk Si<sub>3</sub>N<sub>4</sub>.<sup>22,23</sup>



**Figure 3.** Growth per cycle (GPC) as a function of the precursor dosing time for a table temperature of 100 °C, 200 °C, and 500 °C. The GPC was determined using a 3 s plasma exposure time. The lines serve as a guide to the eye.

small nonideal component or soft saturation behavior. In both Table 1 and Figure 3, a decrease in GPC with increasing temperature was observed. Note that the GPC values in Figure 3 differ from the steady-state GPC values in Table 1, since Figure 3 was obtained using a 3 s plasma instead of a 10 s plasma in the cycle (the needed precursor dose is expected to be only minimally affected by the plasma exposure time). Furthermore, Table 1 shows that the refractive index and mass density increased with temperature, while there was a decrease in the N/Si ratio, C content, and H content. The O content was generally low ( $\leq 5$  at. %). X-ray diffraction (XRD) revealed that all films were amorphous (data not shown), and atomic force microscopy showed that the deposited films were smooth with a low RMS roughness of  $0.3 \pm 0.1$  nm.

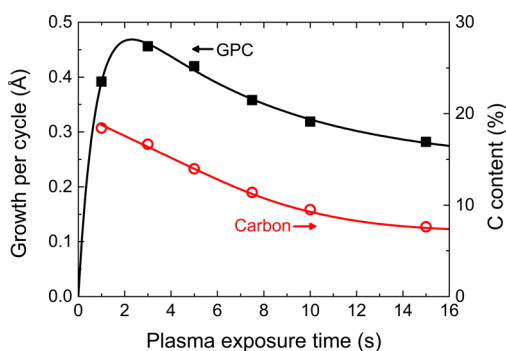


**Figure 4.** GPC and carbon content of the SiN<sub>x</sub> films as a function of plasma exposure time for a table temperature of 200 °C. The lines serve as a guide to the eye.

**Effect of Plasma Exposure.** Figure 4 and Table 2 show the effect of the plasma exposure time on the GPC and the material properties. Figure 4 shows that there was initially a rapid increase in the GPC followed by a slow decrease toward a constant value. Furthermore, there was a continuous decrease in C content with plasma exposure time. Table 2 shows that with longer plasma exposure time there was also an increase in refractive index and a slight increase in O content, which was likely incorporated from background species in the reactor (i.e., a longer plasma exposure leads to a longer exposure of the surface to species present in the background such as oxygen and water). The mass density data for 10 and 15 s plasma exposure time,  $2.2 \pm 0.1$  g/cm<sup>3</sup> and  $2.4 \pm 0.1$  g/cm<sup>3</sup>, respectively, shows an increase of mass density for longer plasma exposure times. The deposition at a lower pressure of 13 mTorr instead of 40 mTorr demonstrated that a decrease in plasma pressure can improve the material properties, i.e., a higher refractive index, a lower N/Si ratio, and low C and O contents were obtained.

Figure 5a shows the refractive index as a function of plasma exposure time, measured directly after deposition and after 1 and 2 months. Films deposited using 7.5 s plasma or longer were stable to oxygen incorporation over this period of time. For shorter plasma times there was a decrease in refractive index over time. Figure 5b and 5c show the XPS depth profiles for films deposited using 3 and 15 s plasma exposure times, respectively. The profiles directly after deposition and 1 month later are shown. Directly after deposition, both films showed a fairly low O content over the film thickness. After 1 month, the film deposited using 3 s plasma exposure showed a much higher O content ( $\sim 50$  at. %) and a relative decrease in N and C content. SE showed that this change was accompanied by a thickness increase from 63.9 to  $84.3 \pm 0.5$  nm and a decrease in refractive index from 1.75 to  $1.53 \pm 0.03$ . The change in material properties and thickness indicates oxidation of the film. The low gradient in O content can be explained by the oxidation having proceeded down to the interface, with no oxidation further occurring. Figure 5c shows that the film deposited using 15 s plasma exposure underwent no observable change in composition. Note that both films were deposited on Si substrates with a native oxide layer, which accounts for the higher O content at the interface between film and substrate. Experiments on HF-dipped Si substrates did not show this higher O content at the interface.

Films were also prepared at room temperature, and for this temperature saturating behavior was also found (Figure S1).<sup>15</sup> The best material properties were obtained for a plasma exposure of 20 s N<sub>2</sub> at 13 mTorr. For this sample, the GPC was  $1.17 \pm 0.02$  Å, and the refractive index was  $1.76 \pm 0.03$

**Table 2.** GPC, Refractive Index, and Composition of SiN<sub>x</sub> Films Deposited Using Different Plasma Exposure Times in the Cycle at 40 mTorr N<sub>2</sub> Pressure and a Table Temperature of 200 °C<sup>b</sup>

plasma exposure time (s)	GPC (Å)	refractive index	XPS			ERD
			N/Si ratio	[C] at. %	[O] at. %	[H] at. %
1	0.39 ± 0.02	1.56 ± 0.03	2.1 ± 0.1	18 ± 1	4 ± 1	-
3	0.46	1.75	2.1	17	3	-
5	0.42	1.78	1.9	14	3	-
7.5	0.36	1.82	1.8	11	4	-
10	0.32	1.83	1.7	9	5	10.9 ± 0.5
15	0.28	1.86	1.7	8	5	9.6
10 <sup>a</sup>	0.24	1.91	1.6	6	5	-

<sup>a</sup>The N<sub>2</sub> plasma pressure was set at 13 mTorr instead of 40 mTorr. <sup>b</sup>Typical error margins are indicated for the first value in each column. A dash indicates “not measured”.

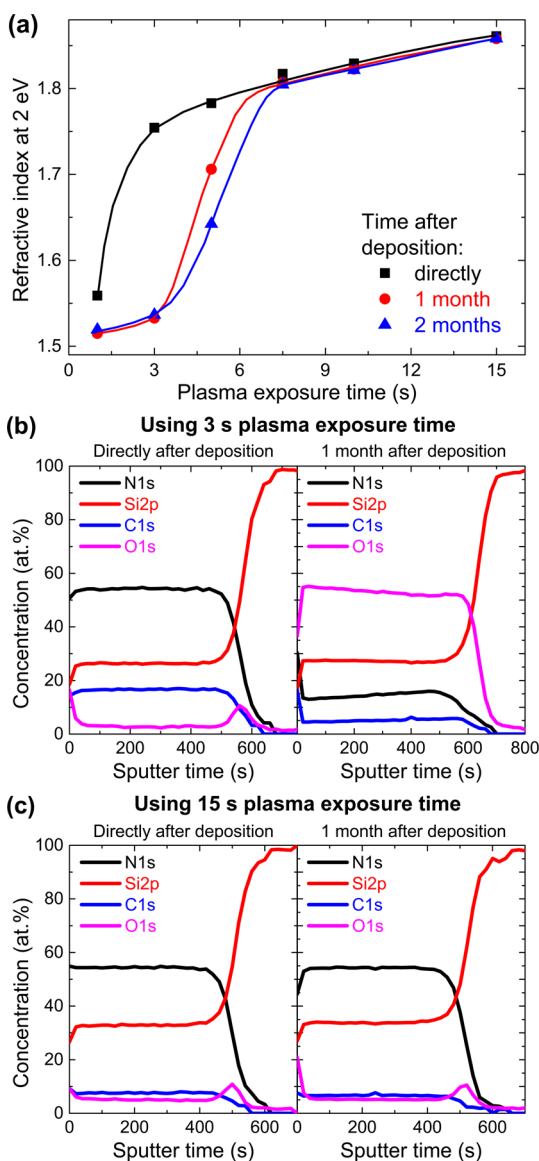


**Figure 5.** (a) The refractive index as a function of plasma exposure time for films analyzed directly after deposition and compared to those of the same films analyzed 1 month and 2 months after deposition. The X-ray photoelectron spectroscopy (XPS) depth profiles measured directly after deposition and 1 month after deposition for a film deposited with a plasma exposure time of 3 s (b) and 15 s (c) are shown. The substrate table temperature was 200 °C.

(determined *in situ*). XPS measurements showed a N/Si ratio of  $2.3 \pm 0.1$ , a C content of  $20 \pm 1\%$ , and an O content of  $2 \pm 1\%$ . Note that the longer plasma exposure and lower pressure used for this film deposited at room temperature led to a higher refractive index, a lower N/Si ratio, and a lower C content than for films prepared at 100 °C under standard conditions. Nevertheless, these films were prone to immediate oxidation on removal from the reactor. An Al<sub>2</sub>O<sub>3</sub> capping layer was deposited *in situ* by ALD onto the SiN<sub>x</sub> film, which prevented this oxidation to the extent that the film composition was the same after 2 months in air as it was directly after deposition.

**Wet-Etch Rates.** Table 3 shows wet-etch rates, from high to low, for a selection of SiN<sub>x</sub> films. The results for a thermal oxide

**Table 3.** Wet-Etch Rates for SiN<sub>x</sub> Films Deposited at Various Table Temperatures and with Different Plasma Times at 40 mTorr N<sub>2</sub> Pressure<sup>b</sup>

table temp (°C)	plasma time (s)	wet-etch rate (nm/min)	
		100:1 HF	7:1 BHF
200	7.5	71 ± 15	-
200	10	28 ± 8	-
200	15	11 ± 4	38 ± 4
200	10 <sup>a</sup>	2.7 ± 0.7	14 ± 2
300	10	1.3 ± 0.7	5.6 ± 0.2
400	10	0.2 ± 0.5	1.1 ± 0.3
500	10	0.0 ± 0.1	0.8 ± 0.2
thermal oxide	0.6 ± 0.1	82.8 ± 0.7	-

<sup>a</sup>The N<sub>2</sub> plasma pressure was set at 13 mTorr instead of 40 mTorr.

<sup>b</sup>Wet-etch rates for thermal oxide are shown in the last row as a reference. A dash indicates “not measured”.

film (400 nm SiO<sub>2</sub>) are given for comparison. The 100:1 HF etch rates of thermal oxide have the same order of magnitude but have a lower value than reported in the literature (e.g., 0.6 nm/min versus 2.3 nm/min).<sup>17</sup> Thermal oxide etch rates for 7:1 BHF were in the range reported in the literature which is between 50 and 100 nm/min.<sup>17</sup> Note that BHF solutions are considered to be more reliable for controlled etching since etching is affected by the acidity of the solution which is more constant in buffered solutions such as BHF.<sup>17</sup>

## DISCUSSION

To obtain SiN<sub>x</sub> films with a composition close to stoichiometric Si<sub>3</sub>N<sub>4</sub> and with low wet-etch rates, the most important parameters were table temperature, plasma exposure time, and plasma pressure. For high table temperatures, properties relatively close to those of bulk Si<sub>3</sub>N<sub>4</sub> were obtained. At 200 °C,

a long plasma exposure time of 15 s or a low plasma pressure of 13 mTorr gave the best material properties and most stable films. The benefit of using lower pressure could be related to ion bombardment (ion energy  $\approx 15$  eV).<sup>11,18</sup> However, as was shown in a recent publication,<sup>19</sup> the effect of faster removal of reaction products from the chamber was more important as it limits the chance of these products to be dissociated and redeposit on the surface. At short plasma exposure times and low table temperatures, impurity levels were high and the films were unstable in air. This could again be related to redeposited species that are not completely removed from the surface or alternatively that ligands were not completely removed during the plasma step. Both these processes would result in a higher carbon content and lower mass density of the films, which would lead to a higher GPC. Incorporation of N from the N<sub>2</sub> plasma on the impurity-containing surface could explain the high N/Si ratio of 2.7 at 100 °C.

When comparing the main results from this work with those from SiN<sub>x</sub> ALD processes reported in the literature, several observations can be made. The first observation is that ALD behavior was investigated over a wider temperature window in this work (even at room temperature), while for instance for chlorosilanes the lowest reported temperature is 225 °C.<sup>4</sup> On the other hand, fairly low GPC values were observed in this work compared to the other processes in the literature, e.g., 0.32–0.15 Å at 200–500 °C compared to 0.65 Å for growth using N(SiH<sub>3</sub>)<sub>3</sub> (TSA) and NH<sub>3</sub> plasma or compared to 2.3 Å for growth using Si<sub>2</sub>Cl<sub>6</sub> and N<sub>2</sub>H<sub>4</sub>.<sup>3,13</sup> This difference could be related to the larger size of the BTBAS precursor. Furthermore, the used precursors have often more than one Si atom per precursor molecule (e.g., TSA has three Si atoms), which can lead to more Si atoms deposited per precursor molecule. The fairly short precursor dosing time of 150 ms might suggest that the reactivity of BTBAS with the surface after N<sub>2</sub> plasma is higher than for other SiN<sub>x</sub> ALD processes. This would be supported by the fact that the required exposure for saturated growth was much lower than that reported for SiH<sub>2</sub>Cl<sub>2</sub> on an NH<sub>3</sub> plasma exposed surface (i.e., < 0.1 Torr·s compared to 1–10 Torr·s).<sup>10</sup> The material quality was remarkably high, taking into account that at a 500 °C table temperature the actual wafer temperature is expected to be more than 100 °C lower.<sup>15</sup> For instance the process from Morishita et al. using Si<sub>2</sub>Cl<sub>6</sub> and N<sub>2</sub>H<sub>4</sub> required a temperature of >525 °C to obtain the same refractive index.<sup>3</sup> The refractive index was also higher than the refractive index obtained for other chlorine-free processes reported, i.e.,  $\leq 1.96$  versus  $\leq 1.85$ , while the films were also nitrogen-rich.<sup>12,13</sup> The latter could be related to the N/Si ratio in the precursor, 2:1 for BTBAS compared to 1:3 for TSA, and it could also be related to the usage of a pure N<sub>2</sub> plasma as the coreactant instead of H-containing coreactants such as NH<sub>3</sub> plasma used by others.<sup>5,7,8,13</sup> Also, a relatively low H content was observed, which is important for the wet-etch rate as will be discussed in the next paragraph.

Table 3 shows that both 0.5% HF and 7:1 BHF wet-etch rates show the same trend for the SiN<sub>x</sub> films, where low etch rates were obtained for films deposited at high table temperatures and for films with lower impurity and hydrogen levels. This is, for instance, revealed by the films deposited at longer plasma time (15 s compared to 10 s) and at lower plasma pressure (13 mTorr versus 40 mTorr). Chow et al. reported etch rates with similar BHF etchant (i.e., 13:2 BHF compared to 7:1 BHF) for SiN<sub>x</sub> films deposited using plasma-enhanced chemical vapor deposition (PECVD) and low-

pressure chemical vapor deposition (LPCVD) and observed that films with low H content had the lowest etch rates. The lowest values were around 1 nm/min for LPCVD Si<sub>3</sub>N<sub>4</sub> films deposited at >700 °C,<sup>20</sup> which is similar to those of the best films in this work (prepared at 400 and 500 °C) with a comparable H content ( $\sim 5\%$ ). Note also that the H content was lower than the 15% reported for LPCVD BTBAS at 550–600 °C.<sup>21</sup> Hence, in comparison to wet-etch rates for other SiN<sub>x</sub> ALD processes, good results were already achieved at relatively low temperatures. Koehler et al. achieved  $\sim 1$  nm/min at 500 °C using a similar etchant (1:100 HF), which were achieved at table temperatures between 300 and 400 °C in this work. The fact that the coreactant was a pure N<sub>2</sub> plasma (i.e., without any H) suggests that H-free plasmas are beneficial for obtaining films with low H content and low wet etch rates.

## CONCLUSIONS

A new ALD process for silicon nitride was developed using bis(*tert*-butylamino)silane (BTBAS) and N<sub>2</sub> plasma. The process exhibited a wide temperature window stretching from room temperature up to 500 °C. The material properties depended strongly on plasma exposure time, plasma pressure, and substrate table temperature. For applications where LPCVD and high-temperature thermal ALD have to be replaced to reduce the thermal budget, table temperatures of 300 to 500 °C would be best for this process. Under these conditions a composition close to Si<sub>3</sub>N<sub>4</sub> was obtained at a table temperature of 500 °C, i.e., a N/Si ratio of  $1.4 \pm 0.1$ , a mass density of  $2.9 \pm 0.1$  g/cm<sup>3</sup>, and a refractive index of  $1.96 \pm 0.03$ . Low buffered HF wet-etch rates of  $\sim 1$  nm/min were obtained for films deposited at table temperatures of 400 and 500 °C, similar to that achieved in the literature using LPCVD Si<sub>3</sub>N<sub>4</sub> at >700 °C. The low H content (i.e.,  $\sim 5\%$ ) of the films is expected to be an important factor for this result.

For applications demanding ALD SiN<sub>x</sub> at lower temperatures, the temperature window from room temperature to 200 °C could be a solution. For these temperatures fairly high material quality was obtained for low plasma pressure or long plasma exposure time (e.g., for deposition at 200 °C using 13 mTorr plasma pressure, the N/Si ratio was  $1.6 \pm 0.1$ , and the refractive index was  $1.91 \pm 0.03$ ). The relatively low precursor doses needed for the presented process could indicate a highly reactive surface after the N<sub>2</sub> plasma that could be beneficial to minimize precursor consumption and facile growth at low temperatures. Future work will focus on studying the conformality of the ALD SiN<sub>x</sub> process and understanding the growth mechanisms.

## ASSOCIATED CONTENT

### Supporting Information

The Supporting Information is available free of charge on the ACS Publications website at DOI: 10.1021/acsami.5b06833.

Table S1 and Figure S1 (PDF)

## AUTHOR INFORMATION

### Corresponding Authors

\*E-mail: h.c.m.knoops@tue.nl.

\*E-mail: w.m.m.kessels@tue.nl.

### Author Contributions

The manuscript was written through contributions of all authors. All authors have given approval to the final version of the manuscript.

## Funding

The research of one of the authors (W.M.M.K.) has been made possible by the Dutch Technology Foundation STW and The Netherlands Organization for scientific Research (NWO, VICI programma, 10817).

## Notes

The authors declare no competing financial interest.

## REFERENCES

- (1) Koehler, F.; Triyoso, D. H.; Hussain, I.; Antonioli, B.; Hempel, K. Challenges in Spacer Process Development for Leading-edge High-K Metal Gate Technology. *Phys. Status Solidi C* **2014**, *11*, 73–76.
- (2) Koehler, F.; Triyoso, D. H.; Hussain, I.; Mutas, S.; Bernhardt, H. Atomic Layer Deposition of SiN for Spacer Applications in High-end Logic Devices. *IOP Conf. Ser.: Mater. Sci. Eng.* **2012**, *41*, 012006.
- (3) Morishita, S.; Sugahara, S.; Matsumura, M. Atomic-layer Chemical-vapor-deposition of Silicon-nitride. *Appl. Surf. Sci.* **1997**, *112*, 198–204.
- (4) Klaus, J.; Ott, A.; Dillon, A.; George, S. Atomic Layer Controlled Growth of Si<sub>3</sub>N<sub>4</sub> Films using Sequential Surface Reactions. *Surf. Sci.* **1998**, *418*, L14–L19.
- (5) Goto, H.; Shibahara, K.; Yokoyama, S. Atomic Layer Controlled Deposition of Silicon Nitride with Self-limiting Mechanism. *Appl. Phys. Lett.* **1996**, *68*, 3257–3259.
- (6) Park, K.; Yun, W.-D.; Choi, B.-J.; Kim, H.-D.; Lee, W.-J.; Rha, S.-K.; Park, C. O. Growth Studies and Characterization of Silicon Nitride Thin Films Deposited by Alternating Exposures to Si<sub>2</sub>Cl<sub>6</sub> and NH<sub>3</sub>. *Thin Solid Films* **2009**, *517*, 3975–3978.
- (7) Yokoyama, S.; Goto, H.; Miyamoto, T.; Ikeda, N.; Shibahara, K. Atomic Layer Controlled Deposition of Silicon Nitride and In Situ Growth Observation by Infrared Reflection Absorption Spectroscopy. *Appl. Surf. Sci.* **1997**, *112*, 75–81.
- (8) Ovanesyan, R. A.; Hausmann, D. M.; Agarwal, S. Low-temperature Conformal Atomic Layer Deposition of SiN<sub>x</sub> Films using Si<sub>2</sub>Cl<sub>6</sub> and NH<sub>3</sub> Plasma. *ACS Appl. Mater. Interfaces* **2015**, *7*, 10806–10813.
- (9) Riedel, S.; Sundqvist, J.; Gumprecht, T. Low Temperature Deposition of Silicon Nitride using Si<sub>3</sub>Cl<sub>8</sub>. *Thin Solid Films* **2015**, *577*, 114–118.
- (10) Murray, C. A.; Elliott, S. D.; Hausmann, D.; Henri, J.; LaVoie, A. Effect of Reaction Mechanism on Precursor Exposure Time in Atomic Layer Deposition of Silicon Oxide and Silicon Nitride. *ACS Appl. Mater. Interfaces* **2014**, *6*, 10534–10541.
- (11) Profijt, H. B.; Potts, S. E.; Kessels, W. M. M.; Van de Sanden, M. C. M. Plasma-Assisted Atomic Layer Deposition: Basics, Opportunities, and Challenges. *J. Vac. Sci. Technol., A* **2011**, *29*, 050801.
- (12) King, S. W. Plasma-enhanced Atomic Layer Deposition of SiN<sub>x</sub>:H and SiO<sub>2</sub>. *J. Vac. Sci. Technol., A* **2011**, *29*, 041501.
- (13) Jang, W.; Jeon, H.; Kang, C.; Song, H.; Park, J.; Kim, H.; Seo, H.; Leskela, M.; Jeon, H. Temperature Dependence of Silicon Nitride Deposited by Remote Plasma Atomic Layer Deposition. *Phys. Status Solidi A* **2014**, *211*, 2166–2171.
- (14) Heil, S. B. S.; Hemmen, J. L.; Hodson, C. J.; Singh, N.; Klootwijk, J. H.; Roozeboom, F.; van de Sanden, M. C. M.; Kessels, W. M. M.; van Hemmen, J. L. Deposition of TiN and HfO<sub>2</sub> in a Commercial 200 mm Remote Plasma ALD Reactor. *J. Vac. Sci. Technol., A* **2007**, *25*, 1357–1366.
- (15) See the [Supporting Information](#) for actual wafer temperatures and saturation curve for growth at room temperature.
- (16) Ande, C. K.; Knoops, H. C. M.; de Peuter, K.; van Druenen, M.; Elliott, S. D.; Kessels, W. M. M. Role of Surface Termination in Atomic Layer Deposition of Silicon Nitride. *J. Phys. Chem. Lett.* **2015**, *6*, 3610–3614.
- (17) Williams, K. R.; Gupta, K.; Wasilik, M. Etch Rates for Micromachining Processing-Part II. *J. Microelectromech. Syst.* **2003**, *12*, 761–778.
- (18) Profijt, H. B.; Kudlacek, P.; van de Sanden, M. C. M.; Kessels, W. M. M. Ion and Photon Surface Interaction during Remote Plasma ALD of Metal Oxides. *J. Electrochem. Soc.* **2011**, *158*, G88–G91.
- (19) Knoops, H. C. M.; de Peuter, K.; Kessels, W. M. M. Redeposition in Plasma-assisted Atomic Layer Deposition: Silicon Nitride Film Quality Ruled by the Gas Residence Time. *Appl. Phys. Lett.* **2015**, *107*, 014102.
- (20) Chow, R. Hydrogen Content of a Variety of Plasma-deposited Silicon Nitrides. *J. Appl. Phys.* **1982**, *53*, 5630–5633.
- (21) Gumphier, J.; Bather, W.; Mehta, N.; Wedel, D. Characterization of Low-Temperature Silicon Nitride LPCVD from Bis(tertiary-butylamino)silane and Ammonia. *J. Electrochem. Soc.* **2004**, *151*, G353–G359.
- (22) Bååk, T. Silicon Oxynitride; a Material for GRIN Optics. *Appl. Opt.* **1982**, *21*, 1069–1072.
- (23) Haynes, W. M. *CRC Handbook of Chemistry and Physics*, 95th ed., 2014–2015; 2014; Vol. 54.

## NOTE ADDED AFTER ASAP PUBLICATION

This paper published ASAP on August 28, 2015. Reference 16 was updated and the revised version was reposted on September 9, 2015.